4D Catalan's Lattice

Gennady Eremin

argenns@gmail.com

February 8, 2018

Abstract. This note shows that well-known the Dyck triangle, the Catalan triangle, and the Catalan convolution matrix are projections of a mutable 4D Catalan's Lattice. By selecting coordinate axes, the Catalan's Lattice can be transformed into 2D and 3D modifications. Paths in some modifications are analyzed.

Key Words: Catalan numbers, Catalan lattice, Dyck triangle, Catalan triangle, Catalan convolution matrix, Dyck path, monotonic lattice path.

Russian version: http://eremin.xyz/catalan_lattice-2018ru.pdf

In discrete mathematics, Pascal's pyramid, a three-dimensional arrangement of the trinomial numbers, is well-known. In this note, we will consider multidimensional constructions somewhat akin to Pascal's pyramid.

1 Introduction

The Catalan numbers appear in many counting problems in combinatorics. The *n*th Catalan number is

$$Cat(n) = \frac{1}{n+1}\binom{2n}{n}, \quad n \geq 0.$$

The first Catalan numbers (n = 0, 1, 2, …) are 1, 1, 2, 5, 42, 132, 429, 1430, … (OEIS A000108). The Catalan numbers enumerate a lot of combinatorial objects [1]. We will be interested in two the simplest and popular species, these are *mountain ranges* (or the *Dyck paths*) and *monotonic lattice paths*.

In Figure 1, a mountain range (the left picture) is formed by upstrokes and downstrokes that stay above the horizontal line. A monotonic lattice path (the right picture) is one along the edges of a grid with square cells which starts in the lower left corner, finishes in the upper right corner, and does not pass above the diagonal.

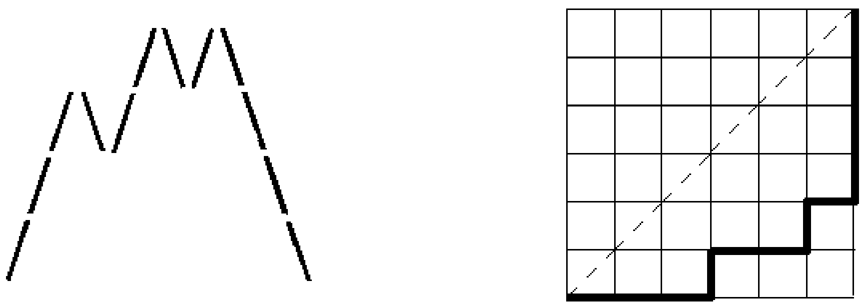

Figure 1: Corresponding Range and Path

The bijection between mountain ranges and lattice paths is obvious. The number of ranges with n upstrokes and n downstrokes is equal to the number of monotonic paths on the n-by-n grid, and is equal to the nth Catalan number. Let's pay attention, mountain ranges have only diagonal links, and lattice paths avoid diagonals. This suggests that between these two objects there is a very close relationship.

2 Isolines of Dyck triangle

Mountain ranges are convenient to draw in the Dyck triangle in the form of the directed Dyck paths. The Dyck path of length $2n$ (or *semilength* n) is a diagonal path from the origin to the node $(2n, 0)$ consisting of n upsteps, vectors $(1, 1)$, and n downsteps, vectors $(1, -1)$. The Dyck path does not fall below the ground level.

Figure 2 shows the directed Dyck path of semilength 6 that corresponds to the mountain range in Figure 1. The relevant balanced parentheses are shown below (a "(" corresponds to the upstep, a ")" corresponds to the downstep).

In Figure 2, the *positions* of the vectors are plotted along the abscissa axis (green), *i-axis*, and the *unbalance*, exceeding the number of upsteps above downsteps, is along the ordinate axis (blue), *j-axis*. In the *i*-by-*j* grid, the *achievable* (*accessible*) points through which the Dyck paths pass are labeled. Unreachable nodes are not shown (omitted).

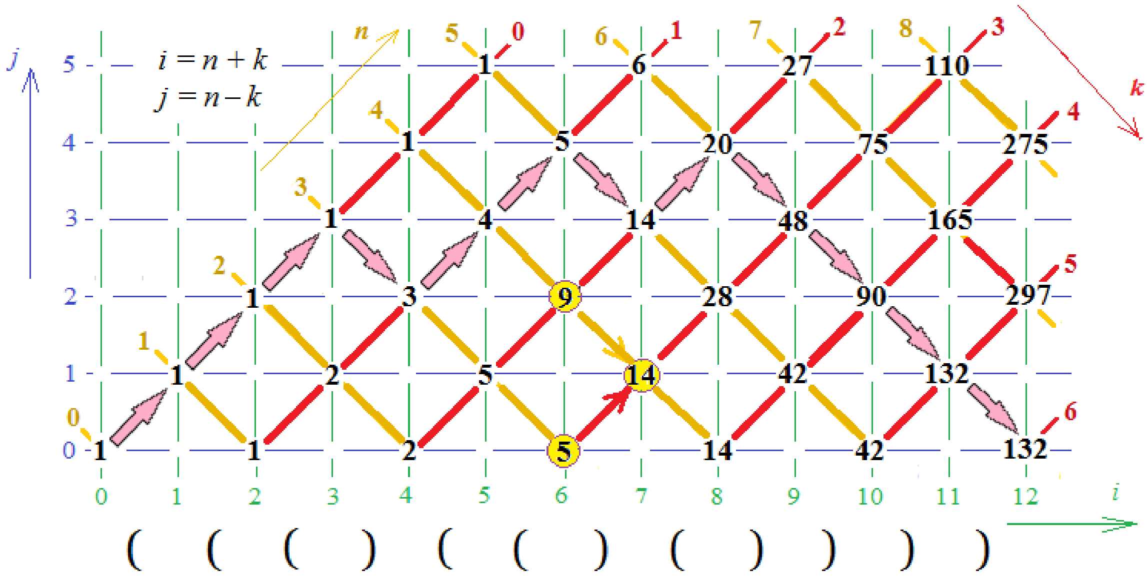

Figure 2: Dyck triangle in the *i*-by-*j* grid.

The accessible node (i, j) has a label (or *dynamics*) $d(i, j)$, which is equal to the number of paths starting at $(0, 0)$ and ending at (i, j). The following *dynamics equation* is valid:

$$d(0, 0) = 1, \;\; d(i, j) = d(i-1, j+1) + d(i-1, j-1). \qquad (1)$$

The dynamics is zero in unreachable nodes. In the bottom two lines, we have the Catalan numbers, that is, $d(2n-1, 1) = d(2n, 0) = \mathrm{Cat}(n)$. In yellow we have identified three nodes connected by (1): $d(7, 1) = d(6, 0) + d(6, 2)$. The path of semilength 6 and these three nodes will be repeated in following figures.

Figure 2 shows horizontal and vertical *isolines*. The horizontal line (blue) is a *j-isoline*, since it passes the points with the same j coordinate. Respectively, the vertical line (green) is an *i-isoline*. But the triangle also has diagonal lines. Let's consider them too.

For the accessible node (i, j), the sum of the coordinates is even, write it like this $i + j = 2n$. This sum is same for all nodes in the falling diagonal (highlighted in yellow), which starts at the top node (n, n) and ends at the bottom node (2n, 0).

In the falling diagonal, the bottom node is labeled with a Catalan number, so it is logical to relate the falling diagonal, further *n-isoline*, to the index of a Catalan number. In Figure 2, the selected nodes (6, 2) and (7, 1) are at the n-isoline #4, so we assume that these points are tied to $Cat(4)$.

For the accessible node (i, j), the coordinate difference is also even, write it like this $i - j = 2k$. This difference is same for all nodes in the rising diagonal (highlighted in red), which starts at the node (2k, 0). The rising diagonal will be called a *k-isoline*. The main diagonal of the i-by-j grid is the k-isoline #0. The selected nodes (6, 0) and (7, 1) are at the k-isoline #3.

Thus, the accessible node (i, j) is at the intersection of four isolines: (1) the i-isoline #i (vertical), (2) the j-isoline #j (horizontal), (3) the n-isoline number $n = (i + j)/2$ (falling diagonal), and (4) the k-isoline number $k = (i - j)/2$ (rising diagonal). We will write this in the form of equalities:

$$i + j = 2n,\ i - j = 2k \quad \text{or} \quad i = n + k,\ j = n - k \quad (i \geq n \geq j,\ n \geq k). \tag{2}$$

Let's pay attention, in (2) *four variables are equal* (*equivalent*): any pair defines another pair. This allows you to build other grids. For example, in Figure 1, the monotonous lattice paths (the right picture) are drawn in the n-by-k grid.

Therefore, we can call the expression (2) *coordinate equations*, and we reproduced these equations in Figure 2 (upper left corner). The yellow arrow shows the direction of the virtual n-axis, and the red arrow shows the direction of the virtual k-axis.

So, we are dealing with some construction in the i-by-j-by-n-by-k grid (further we will try to follow this order of the axes). As a result, we can rewrite (1) in the form of the *generalized dynamics equation*

$$D(0, 0, 0, 0) = 1,\ D(i, j, n, k) = D(i-1, j-1, n-1, k) + D(i-1, j+1, n, k-1). \tag{3}$$

Respectively, for the selected three nodes, we obtain $D(7, 1, 4, 3) = D(6, 0, 3, 3) + D(6, 2, 4, 2)$.

In Figure 2, the Dyck path of semilength 6 starts at the origin (0, 0, 0, 0) and ends at the point (12, 0, 6, 6). The upsteps lie on the k-isolines (n increases, k constant), and the downsteps lie on the n-isolines (n constant, k increases). This situation is identical for each path in any grid (for example, see right picture in Figure 1).

Definition: *Catalan's Lattice is a set of accessible nodes connected by n-isolines and k-isolines.*

In the i-by-j grid, Catalan's Lattice is the Dyck triangle. However, with the help of equations (2) we can modify (or transform) Catalan's Lattice by changing the coordinate system. Recall again the monotonous paths in Figure 1. Moreover, each modification of Catalan's Lattice can be regarded as a self-sufficient copy (or "reincarnation").

Changing the coordinates you can easily move from an arbitrary modification of Catalan's Lattice to any other. And this other modification may be, for example, three-dimensional and even four-dimensional. Why not?

Figure 2 shows the 2D modification of Catalan's Lattice in the *i*-by-*j* grid, or *ij-lattice*. In each modification, the list of axes is important, and not their order. For example, we will assume that the *ij*-lattice and the *ji*-lattice are identical. So, Catalan's Lattice has $\binom{4}{2} = 6$ two-dimensional modifications, $\binom{4}{3} = 4$ three-dimensional modifications, and one 4D modification.

3 Two-dimensional modifications of 4D Catalan's Lattice

We will not consider all 2D modifications of Catalan's Lattice (in [2] the reader can look at all six grids). One projection has already been analyzed, and then we selected three more grids:

a) The *n*-by-*k* grid with monotonic paths without diagonals sections (opposite to the diagonal Dyck paths).

b) The *n*-by-*j* grid in which the paths pass both the diagonal sections and along the edges of the cells. In this case Catalan's Lattice is Catalan convolution matrix.

c) The *k*-by-*j* grid in which all nodes are reachable. This is the only 2D modification of Catalan's Lattice that is not triangular.

3.1. Monotonic lattice paths in the *n*-by-*k* grid.

In Figures 2, at the node (i, 0) (or generalized node (i, 0, n, n)), the virtual coordinates are the same, that is, $n = k$ (recall $j = n - k$). Hence in the *n*-by-*k* grid, the *j*-isoline #0 must be the main diagonal with Catalan numbers. Let's transform Figure 2. We twirl the triangle around the main diagonal 180 degrees and then rotate clockwise by 45 degrees. As a result, we formed the *nk*-lattice (see Figure 3).

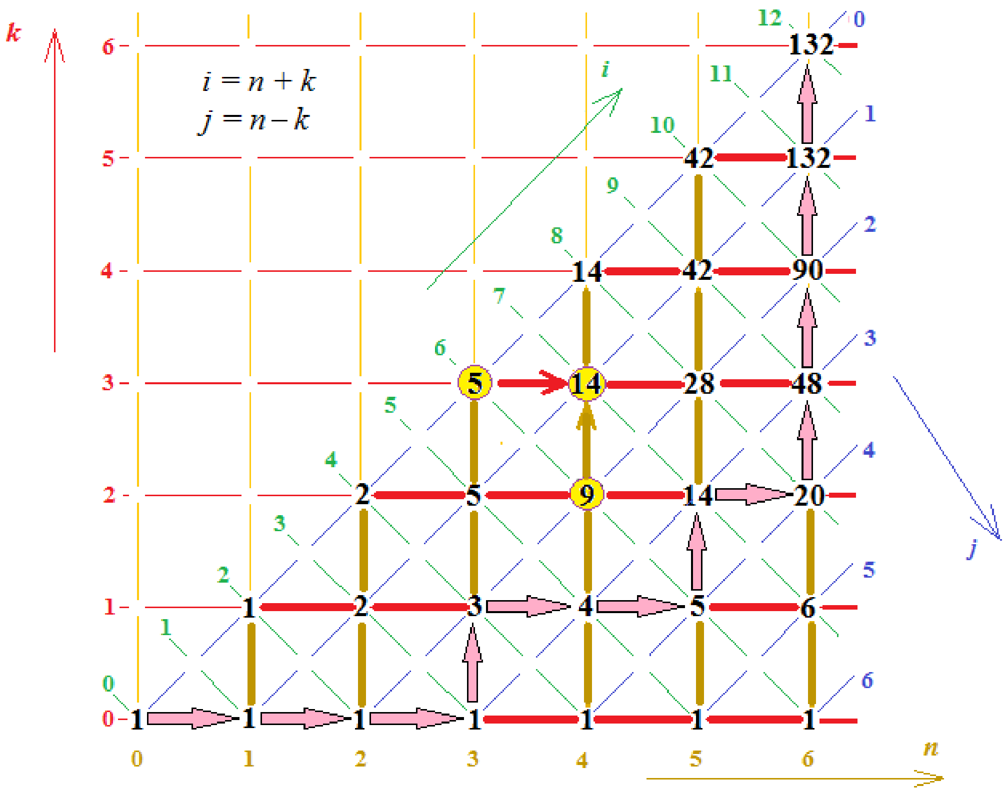

Figure 3: Monotonic lattice paths in the *n*-by-*k* grid.

In a new modification, *i*-isolines and *j*-isolines are virtual (the green arrow and the blue arrow indicate the direction of the virtual axes). At the intersection of virtual isolines, unreachable nodes are omitted (as well as in Figure 2).

In Figure 3, we repeated the previous path of semilength 6 and showed the same three selected nodes. Let’s repeat the corresponding equation $D(7,1,4,3) = D(6,0,3,3) + D(6,2,4,2)$.

3.2. Catalan convolution matrix in the *n*-by-*j* grid.

In Figure 2, let's rotate *n*-isolines to the vertical position around the top points; as a result, we receive the new modification of Catalan’s Lattice in the *n*-by-*j* grid (see Figure 4). We have shown dotted virtual *i*-isolines; the green arrow indicates the direction of the virtual *i*-axis.

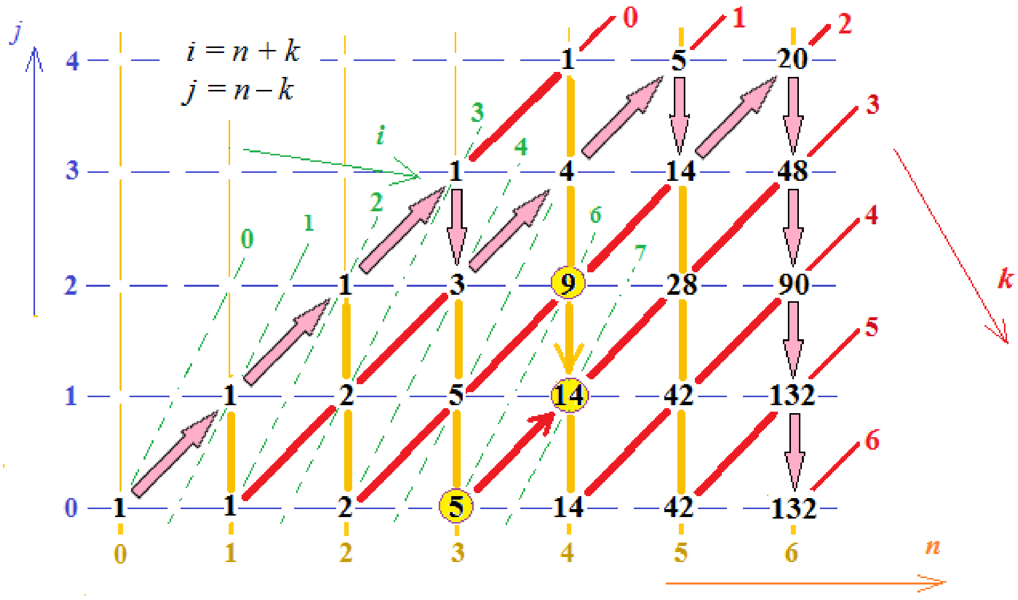

Figure 4: Catalan convolution matrix in the *n*-by-*j* grid.

The former path has significantly changed: upsteps remained the same, and the downsteps are transformed into breaks (throws down). Here, three selected nodes are also shown. For the point (7, 1, 4, 3), the equation of dynamics does not change, and we do not repeat it any more.

In the literature, the *nj*-lattice is known as the Catalan convolution matrix [3, 4]. For its elements, we write the equality from [4, p. 2928] (the variables are indicated in accordance with Figure 4):

$$C_{nj} = \binom{2n-j}{n-j} - \binom{2n-j}{n-j-1}.$$

Using coordinate equations (2), we replace the variables and rewrite the equation in a simplified and general form:

$$D(i, j, n, k) = \binom{i}{k} - \binom{i}{k-1}.$$

3.3. Catalan's Lattice in *k*-by-*j* grid. The modifications considered above have a triangular form. In the *k*-by-*j* grid, the situation is different. Let us return to equalities (2). Four variables are related as follows:

$$i \geq n \geq j \text{ and } n \geq k.$$

As we see, j and k are not connected by inequalities; therefore these variables do not depend on each other. This means that in the *k*-by-*j* grid Catalan's Lattice is not triangular.

Below in Figure 5, we see that the entire first quadrant of the *k*-by-*j* grid is available to paths (there are no forbidden areas). You can observe the virtual unreachable points that arise when *j*-isolines intersect with virtual *i*-isolines (green dotted lines).

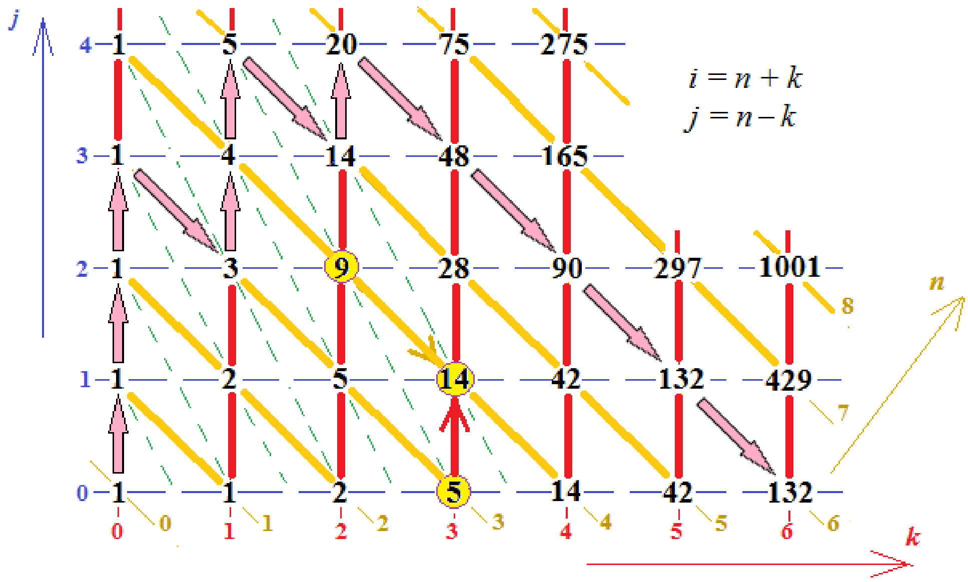

Figure 5: Catalan's Lattice in the *k*-by-*j* grid.

Note that the mentioned unreachable virtual points do not belong to the *k*-by-*j* grid. In this modification, the path of semilength 6 and three selected nodes are also repeated.

4 Three-dimensional modifications of 4D Catalan's Lattice

Recall, there are four three-dimensional modifications of Catalan's Lattice (the order of the axes does not matter). These modifications are cumbersome and we will select only one of them, in our opinion the most promising. If desired, the reader can look at all 3D modifications in [2].

It is convenient to create a 3D modification based on some 2D modification by adding the third axis. It is easy to see that the linear equations (2) ensure the obtaining of 3D flat figures. Presumably, the modification in 4D space (*i*-by-*j*-by-*n*-by-*k* grid) is also flat.

For a better orientation in the three-dimensional space, we will mark axes and different isolines both in space and inside Catalan's Lattice by indicating all four coordinates (three real and one virtual).

In some isolines, there are coincident coordinates. In such cases, the initial coordinates are repeated. Here are a few examples:

$(i, 0, 0, 0)$, $(0, j, 0, 0)$, $(0, 0, n, 0)$, $(0, 0, 0, k)$ – axes in the 4D space;
$(i, i, i, 0)$ – the central ray (*k*-isoline #0), i. e. a set of the points with coordinates $i = j = n$;
$(i, 0, n, n)$ – the main diagonal in the *n*-by-*k* grid (see *j*-isoline #0 in Figure 3).

The isolines are shown as possible in different color: *i*-isolines in green, *j*-isolines in blue, *n*-isolines in yellow, and *k*-isolines in red.

Figure 6 show the *jnk*-lattice that is obtained from the *n*-by-*k* grid. In *j*-by-*n*-by-*k* grid, we repeat the path of semilength 6 and the three nodes (6, 0, 3, 3), (6, 2, 4, 2), (7, 1, 4, 3). As we see this modification of Catalan's Lattice is also flat.

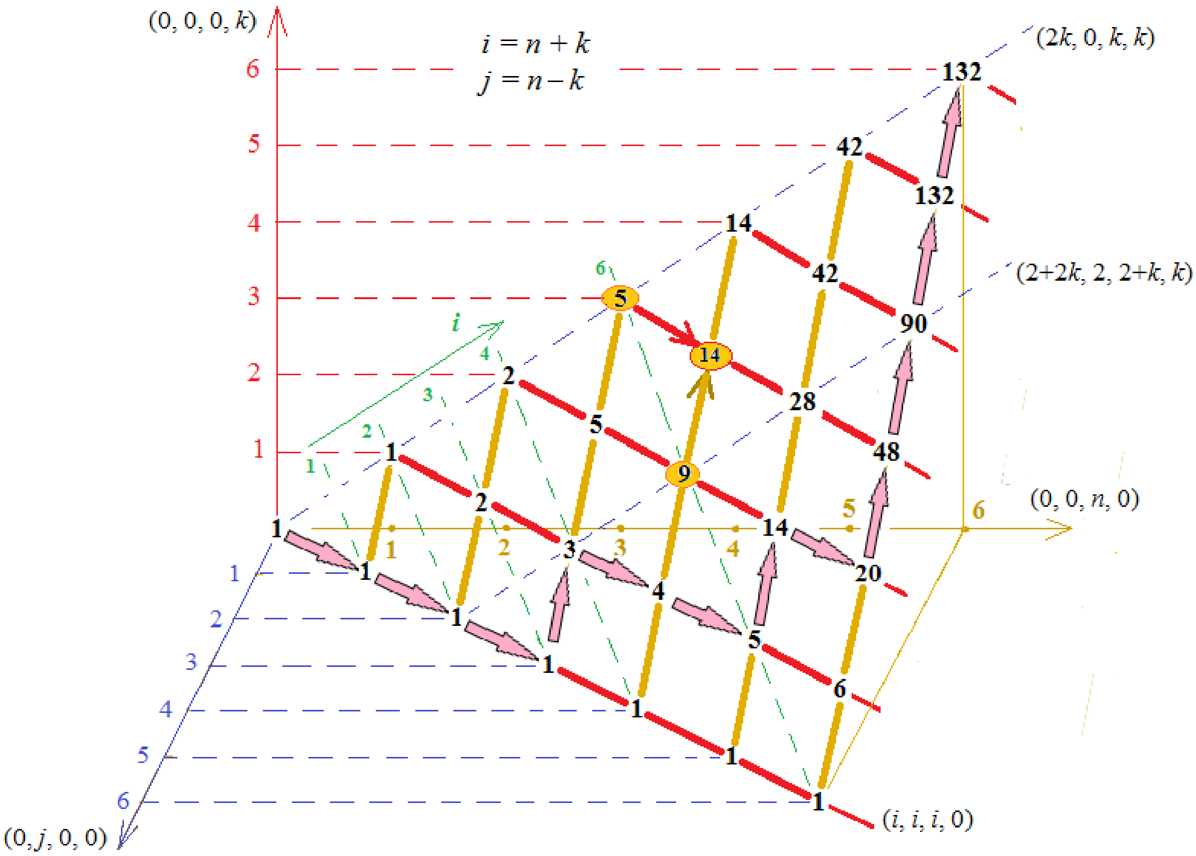

Figure 6: Catalan's Lattice in the *j*-by-*n*-by-*k* grid.

In Figure 6, we conditionally showed the direction of the virtual *i*-axis and some *i*-isolines. Perhaps this picture is most convenient to build a four-dimensional design. (Now this task is beyond the author's power.)

References

[1] R. P. Stanley, *Catalan Numbers*, Cambridge University Press, 2015. http://www.cambridge.org/ro/academic/subjects/mathematics/discrete-mathematics-information-theory-and-coding/catalan-numbers?format=HB

[2] G. Eremin, *Dynamics of Balanced Parentheses, II.4D Dyck Triangle and Its Projections*. http://eremin.xyz/dd2-4D_Dyck_triangle-2017.pdf

[3] Verner E. Hoggatt, Jr., Marjorie Bicknell, *Pascal, Catalan, and General Sequence Convolution Arrays in a Matrix*, *The Fibonacci Quarterly* 14, no. 2 (1976), 135–142. http://www.fq.math.ca/Scanned/14-2/hoggatt2.pdf

[4] David Callan, Emeric Deutsch, *The Run Transform*, *Discrete Mathematics*, **312** (2012), 2927-2937. http://www.sciencedirect.com/science/article/pii/S0012365X12002233